Bulletin of the Seismological Society of America, Vol. 92, No. 8, pp. 2983–2993, December 2002

The Upper-Truncated Power Law Applied to Earthquake Cumulative Frequency–Magnitude Distributions: Evidence for a Time-Independent Scaling Parameter

by S. M. Burroughs and S. F. Tebbens

Abstract Earthquake cumulative frequency–magnitude (CFM) distributions are described by the Gutenberg–Richter power law where the exponent is the *b*-value. Although it has been reported that the *b*-value changes before large earthquakes, we find that an upper-truncated power law applied to earthquake CFM distributions yields a time-independent scaling parameter, herein called the α-value. We analyze earthquakes associated with subduction of the Nazca plate beneath South America and find a region of isolated seismic activity at depths greater than 500 km between 20° S and 30° S. For the entire record, 1973–2000, the earthquake CFM distribution in this isolated region is well described by a Gutenberg–Richter power law with $b = 0.58$. The data set includes several large seismic events with $m_b \geq 6.8$. A power law applied to the CFM distributions for short time intervals between the large events yields *b*-values greater than the *b*-value for the entire record. CFM distributions for the short time intervals are better described by an upper-truncated power law than by a power law. The α-value determined by applying an upper-truncated power law to the short time intervals is equal to the *b*-value obtained by applying the Gutenberg–Richter power law to the entire record. Temporal changes in *b*-value are due to temporal fluctuations in maximum magnitude. Analysis of four Flinn–Engdahl regions, two in subduction zones and two along spreading ridges, demonstrates wider applicability of the results. The α-value is an unchanging characteristic of the system that may be determined from a short-term record.

Introduction

Variations in *b*-value have been reported before major earthquakes. In the years preceding large earthquakes, an increase in *b*-value has been reported in Venezuela (Fiedler, 1974), New Zealand (Smith, 1981, 1986), and the eastern India–Myanmar border region (Sahu and Saikia, 1994). In some studies, a decrease in *b*-value has been reported prior to large earthquakes (Guha, 1979; Molchan and Dmitrieva, 1990; Imoto, 1991; Molchan *et al.*, 1999). Smith (1981) noted that the *b*-value determined from small samples is a statistical parameter related to the mean magnitude of the sample and is not appropriate for long-term prediction. We identify a time-independent scaling parameter that may be determined from a small sample and yet is appropriate for long-term prediction.

Scaling Relationships

Cumulative frequency–magnitude (CFM) distributions of earthquakes are generally described by the Gutenberg–Richter relationship,

$$\log_{10} N = a - b\,m, \tag{1}$$

where N is the number of earthquakes of magnitude greater than or equal to m, b is the scaling exponent, and a is the activity level, which is equal to the log of the number of earthquakes of magnitude $m \geq 0$ (Gutenberg and Richter, 1949). The *b*-value is one of the most important statistical parameters of seismology and is used for probabilistic forecasting.

Aki (1965) developed a maximum likelihood method for determining the *b*-value where

$$b = \frac{\log_{10} \mathrm{e}}{\bar{m} - m_o} \tag{2}$$

and the 95% confidence limit is

$$\delta b = \frac{1.96b}{\sqrt{n}}. \tag{3}$$

The term $\overline{m}$ is mean earthquake magnitude above the threshold magnitude m_o, and n is the number of earthquakes. A similar relationship for b was derived by Utsu (1965). This method has been widely applied (e.g., Oncel *et al.*, 2001) and will be demonstrated using several data sets within this work.

Other functions have been used to describe earthquake distributions. Page (1968) considered a power law distribution over a limited range, setting minimum and maximum values to the noncumulative frequency–magnitude distribution. A power law with an exponential rolloff has been used to describe earthquake CFM distributions that fall away from a power law at large magnitudes (Kagan, 1993; Main, 2000). Bender (1983) demonstrated that the entire CFM distribution is affected by the addition of a large earthquake and that a CFM distribution may fall off from a power law at large event sizes. Similar fall-off patterns have been produced by a nonconservative cellular automaton model for earthquakes (Main *et al.*, 1994; Olami *et al.*, 1992). Cosentino *et al.* (1977) described the fall-off of a CFM distribution when there is a physical limit to the maximum possible magnitude. Field *et al.* (1999) and the Working Group on California Earthquake Probabilities (WGCEP) (1995) used a truncated CFM distribution of moment magnitudes to determine regional b-values in southern California, but temporal changes in b-value were not considered. We develop an equation that describes an earthquake CFM distribution when the power law is abruptly truncated at large magnitude.

A power law applied to a cumulative distribution has the form

$$N(r) = Cr^{-\alpha}, \tag{4}$$

where $N(r)$ is the number of objects with size greater than or equal to r, α is the scaling exponent (the slope on a log–log plot), and C is a constant equal to the number of objects with size $r \geq 1$. In this work, the term frequency refers to the cumulative number of earthquakes, denoted N, as opposed to the number of earthquakes per year, denoted $\dot{N}$. Taking the log of both sides of equation (4), we obtain

$$\log N = \log C - \alpha \log r. \tag{5}$$

Equation (5) has the same form of the Gutenberg–Richter power law, equation (1), where $a = \log C$, $m = \log r$, and $b = \alpha$.

An upper-truncated power law describes cumulative frequency–size distributions associated with several natural systems (Burroughs and Tebbens, 2001b). An upper-truncated power law has the form

$$N_T(r) = C\left(r^{-\alpha} - r_T^{-\alpha}\right), \tag{6}$$

where $N_T(r)$ is the number of objects with size greater than or equal to r, C is the activity level equal to the number of objects of size $r \geq 1$, there are no objects of size r_T or larger, and α is the scaling exponent (Burroughs and Tebbens, 2001a). Since each number of objects in a cumulative distribution includes all larger objects, upper truncation of the distribution decreases the cumulative number associated with each object size. In equation (6), the subtracted term, $Cr_T^{-\alpha}$, represents this decrease from the power law, $Cr^{-\alpha}$.

Applying the upper-truncated power law to earthquake magnitudes, $C = 10^a$, $r = 10^m$, and $r_T = 10^{m_T}$. Substituting into equation (6), the resulting equation for an upper-truncated power law applied to earthquake magnitudes is

$$N_T(m) = 10^a\left((10^m)^{-\alpha} - (10^{m_T})^{-\alpha}\right). \tag{7}$$

Equation (7) provides a quantitative description of the fall-off in the earthquake CFM distribution observed by Bender (1983) and is equivalent to the equation used by Field *et al.* (1999) to study earthquake moment magnitudes. We use equation (7) to analyze several earthquake CFM distributions.

When applying equation (7) to a data set, the Aki (1965) maximum likelihood method for determining the parameters is not appropriate. The Aki method depends on the CFM distribution following a power law with a constant slope on a log–log plot. The slope of an upper-truncated power law is not constant. We find the parameters for equation (7) by minimizing chi-square. The 95% confidence limit is determined by using the residuals to calculate the standard deviation of the parameter and then applying the Student's t-test to determine the confidence limit. This method of determining confidence limits assumes that the errors in fitting the function to the data points are normally distributed with zero mean.

Analysis

To analyze temporal change in b-value, we seek seismic regions that satisfy three criteria. First, we seek regions of isolated seismicity. We thereby avoid the difficulties and errors that may be introduced when arbitrarily selecting boundaries within active seismic regions. Second, we seek regions where several large earthquakes occurred so that we may analyze how large earthquakes affect CFM distributions. Third, the seismic record for the region must contain a sufficient number of reliably recorded earthquakes to analyze CFM distributions between the large events. The only tectonically driven seismic region we found that satisfies all three criteria is along the west coast of South America. Earthquakes in this region are associated with subduction of the Nazca plate beneath the South American plate. A region of isolated seismic activity is found between 20° S and 30° S at depths greater than 500 km (Fig. 1). We use the U.S. Geological Survey/National Earthquake Information Center Preliminary Determination of Epicenters (USGS/NEIC PDE) catalog to analyze earthquakes in this region.

In this study region, we find four large seismic events, labeled E1–E4 (Fig. 2), which are earthquakes of magnitude

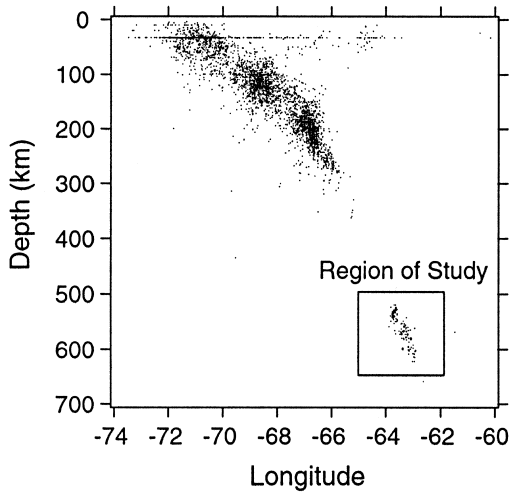

Figure 1. Earthquakes associated with subduction of the Nazca plate beneath South America between 20°S and 30°S from 1973 to 2000. An aseismic region separates shallow and intermediate earthquakes from the deepest earthquakes. We analyze the deep earthquakes (>500 km) outlined by the box.

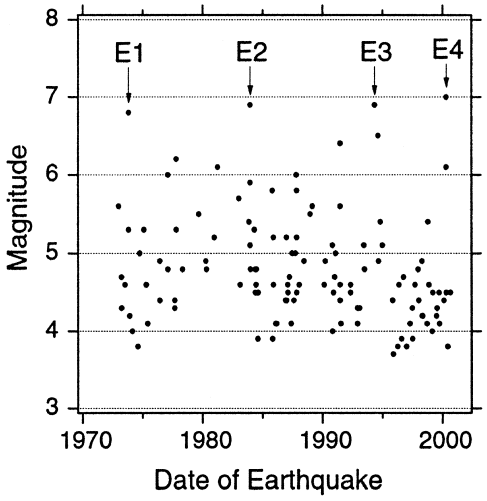

Figure 2. Magnitudes and dates of the earthquakes within the study region shown in Figure 1. Earthquakes of m_b >6.5 are labeled E1, E2, E3, and E4. Event E3 consists of two earthquakes, 11 days apart, each of magnitude m_b 6.9.

6.8, 6.9, and 7.0, respectively. E3 consists of two earthquakes, 11 days apart, each of magnitude 6.9. The largest unlabeled earthquake is magnitude 6.5. The CFM distribution of earthquakes for the entire record, 1973–2000, is well described by the Gutenberg–Richter power law with a b-value of 0.58 ± 0.02 (Fig. 3). The b-value is determined by minimizing chi-square and the 95% confidence limit is reported. Results for this and other CFM distributions are summarized in Table 1. The determined b-value is lower than typical b-values but is consistent with low b-values observed for deep seismic regions (e.g., Kagan, 1991). To examine the temporal change in earthquake CFM distributions, we examine the seismic record between large events (method 1) and for various time intervals preceding large events (method 2).

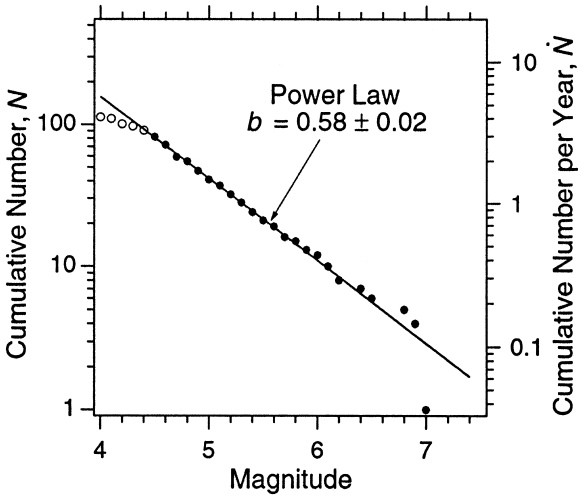

Figure 3. Cumulative frequency–magnitude distribution for all earthquakes in the study region. A Gutenberg–Richter power law describes this distribution and yields a b-value of 0.58 ± 0.02 and a = 4.5. The smallest earthquakes in the record are not used in determining the Gutenberg–Richter b-value and are indicated by open circles.

Method 1

To examine how CFM distributions are affected by a large earthquake, we choose three time intervals bounded by the largest events shown in Figure 2. Each interval begins immediately after a large event and ends at the next large event. First, we examine the time interval bounded by E1 and E2. The CFM distribution for this interval is shown both preceding and including the final event E2 (Fig. 4a). The CFM distribution for events before E2 is fit with an upper-truncated power law, equation (7), yielding an α-value of 0.57 ± 0.22. We set b in equation (1) equal to this α-value and plot the resulting power law (GR PL with b = 0.57, Fig. 4a). The CFM distribution for events including E2 is well described by this power law (Fig. 4a).

Next we examine the time interval bounded by E2 and E3 (Fig. 4b). The CFM distribution for events before E3 is fit with an upper-truncated power law yielding α = 0.68 ± 0.10. The CFM distribution for events including E3 is well described by a power law, equation (1), with b set equal to the determined α-value of 0.68.

Finally, we examine the time interval bounded by E3 and E4 (Fig. 4c). We begin this interval after a possible aftershock of magnitude m_b 6.5 that occurred three months after E3. This interval is shorter than the two preceding intervals and contains few intermediate size earthquakes, making it difficult to obtain a well-constrained α-value when fitting an upper-truncated power law. We include as guide-

Table 1
Summary of Results

Region	Figure	Time Interval	a	α or b	m_T
Chile Trench (All)	3	1973–2000	4.51 ± 0.07	0.58 ± 0.02	
Chile Trench (E2)	4a	1973–1984	3.99 ± 0.99	0.57 ± 0.22	6.72 ± 0.87
Chile Trench (E3)	4b	1984–1994	4.65 ± 0.42	0.68 ± 0.10	6.88 ± 1.05
F-E 410	7.a2	1973–2001	8.44 ± 0.61	1.23 ± 0.12	5.94 ± 0.09
F-E 49	7.b2	1973–2001	9.80 ± 1.30	1.58 ± 0.26	5.88 ± 0.22
F-E 221	7.c2	1973–1994	8.80 ± 0.15	1.22 ± 0.03	6.60 ± 0.12
F-E 189	7.d2	1973–2001	9.19 ± 0.02	1.41 ± 0.14	
Piton de la Fournaise	8	1988–1992	3.67 ± 0.01	0.74 ± 0.02	3.29 ± 0.02

95% confidence limits are reported.

lines on Figure 4c an upper-truncated power law and a Gutenberg–Richter power law. The guidelines were obtained by setting $\alpha = 0.58$, the b-value for the entire data set, and adjusting a and m_T to obtain the best fit of the upper-truncated power law to the distribution of events preceding E4 (lower dashed line, Fig. 4c). These values for a and α were also used to plot the power law guideline (upper dashed line, Fig. 4c). The CFM distribution for the interval preceding E4 is in agreement with the upper-truncated power law guideline with $\alpha = 0.58$.

In summary, for all three time intervals, the CFM distribution preceding the large event is well described by an upper-truncated power law with scaling exponent α. The occurrence of the terminating large event adds one event to each value in the CFM distribution, moving each point in the distribution closer to the power law and decreasing the slope of the distribution. When the terminating event is included, for each time interval the distribution is well described by a power law, equation (1), with scaling exponent b set equal to α.

Method 2

To examine how earthquake CFM distributions change through time, we consider all earthquakes that occurred in progressively shorter time intervals preceding each large event. For E4, we plot the CFM distributions for all earthquakes that occurred in the 25-, 15-, 10-, 5-, and 1-year time intervals immediately preceding E4 (Fig. 5a). Since shorter records are available preceding the remaining large events, the interval durations have been adjusted. We examine the 22-, 15-, 10-, 5-, and 2-year time intervals preceding E3 (Fig. 5b) and the 11-, 5-, and 1-year time intervals preceding E2 (Fig. 5c). A power law is shown as a guideline with $b = 0.58$, equal to the b-value determined for the entire record. Also shown is an upper-truncated power law with $\alpha = 0.58$. An increase in slope of the CFM distribution, corresponding to an increase in b-value, is apparent for the progressively shorter time intervals immediately preceding each large event. An upper-truncated power law with a single α-value describes the CFM distributions for the shortest time intervals preceding all three large events ($\alpha = 0.58$, Fig. 5a–c). This α-value is equal to the b-value of the Gutenberg–Richter power law that describes the entire data set.

Discussion

Upper-Truncated Power Laws

The effects of upper truncating a power law CFM distribution are shown in Figure 6. We start with a Gutenberg–Richter power law, equation (1), and arbitrarily set $a = 8$ and $b = 1.0$ (line PL, Fig. 6). Choosing truncation magnitudes, m_T, equal to 5, 6, and 7, and setting α equal to b, we plot each associated upper-truncated power law, equation (7), as lines A, B, and C, respectively (Fig. 6a). The upper-truncated power law falls off from a power law near the truncation magnitude, producing an increase in slope. This behavior is observed when applying analysis method 1 to the South American study region.

Next, we hold the truncation magnitude and α-value constant and change the activity level. We arbitrarily set $m_T = 6$ and $\alpha = 1.0$. Choosing activity levels, a, equal to 6, 7, and 8, we plot each associated upper-truncated power law as lines D, E, and F, respectively (Fig. 6b). As activity level increases the slope again increases near the truncation magnitude.

Finally, we change both the activity level, a, and the truncation magnitude, m_T, while holding the α-value constant at $\alpha = 1$. Setting a to values of 5, 6, and 7, while simultaneously setting m_T to values of 4, 5, and 6, we plot each associated upper-truncated power law as lines G, H, and I, respectively (Fig. 6c). The upper-truncated power law again has a steeper slope than the power law near the truncation magnitude. This behavior is observed when applying analysis method 2 to the South American study region. All truncated lines plotted in Figure 6 have the same α-value, equal to the b-value of the Gutenberg–Richter power law.

Evidence for a Time-Independent Scaling Parameter

Method 1 examines earthquake CFM distributions in time intervals bounded by the largest events. The earthquakes in the intervals preceding E2 and E3 are well described by an upper-truncated power law (Figs. 4a, 4b). A

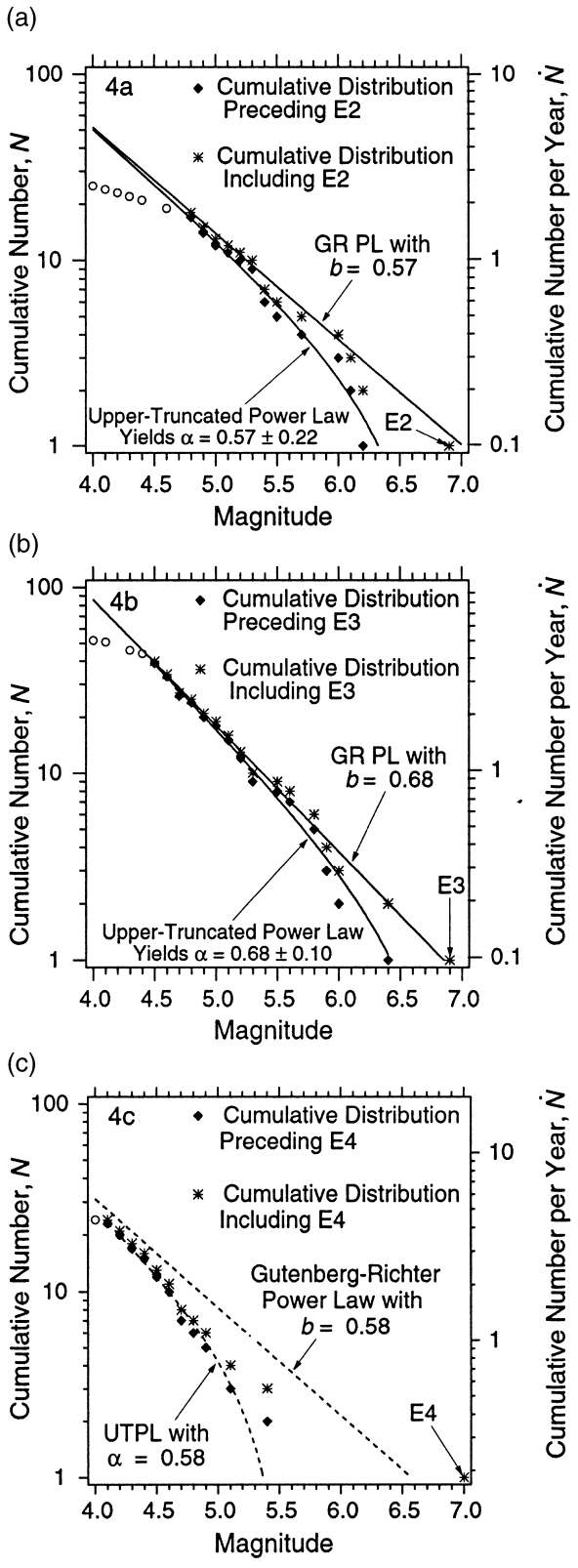

Figure 4. Cumulative frequency–magnitude (CFM) distributions for earthquakes occurring between the events labeled in Figure 2. Open circles are not used in analysis. (a) Beginning immediately after E1 and ending just before E2, the CFM distribution (diamonds) is fit with an upper-truncated power law, equation (7), yielding $\alpha = 0.57 \pm 0.22$ and $a = 4.0$. A Gutenberg–Richter power law, equation (1), with $b = 0.57$ and $a = 4.0$, is shown for comparison (labeled GR PL). When $N = 1$, this power law approximates the magnitude of E2. Stars show the CFM distribution with E2 included. (b) A similar analysis of earthquakes between E2 and E3. In this case, fitting an upper-truncated power law to the cumulative distribution of events preceding E3 yields $\alpha = 0.68 \pm 0.10$ and $a = 4.6$. A power law with these values for α and a approximates the size of E3. (c) The cumulative distribution of events for the time interval between E3 and E4. A power law and an upper-truncated power law (UTPL), each with scaling exponent 0.58, the b-value for the entire record, are shown with dashed lines. For all three intervals between events, the CFM distributions are consistent with an upper-truncated power law.

Gutenberg–Richter power law fit to these distributions would have a steeper slope and therefore a larger b-value than was determined for the entire record. Thus, the b-value for this region exhibits temporal variation due to temporal fluctuations in maximum magnitude. Increases in b-value can be explained by upper truncation of the distribution. Figure 6a demonstrates that an upper-truncated power law has a steeper slope near the truncation magnitude than a power law with the same scaling exponent. The upper truncation observed between large events has a simple explanation: the large terminating event is missing from the interval. The α-value of the upper-truncated power law applied to a short record yields the b-value of the Gutenberg–Richter power law applied to the entire record.

Method 2 examines earthquake CFM distributions in progressively shorter time intervals preceding each large event. The earthquakes in time intervals preceding E2, E3, and E4 are found to have CFM distributions that are steeper for the shorter time intervals immediately preceding the large event (Fig. 5). The longest record precedes E4, where a temporal change in the slope of the CFM distributions is most apparent. A Gutenberg–Richter power law fit to these steeper distributions would demonstrate a temporal increase in b-value as the time intervals become shorter. An upper-truncated power law describes these distributions with a single scaling exponent, the α-value. The observed CFM distributions are replicated by changing both the truncation magnitude and the activity level of the upper-truncated power law, as shown in Figure 6c. Decreases are expected in both activity level and truncation magnitude of earthquake distributions for progressively shorter time intervals. The activity level decreases because there are fewer earthquakes within shorter time intervals. The truncation magnitude de-

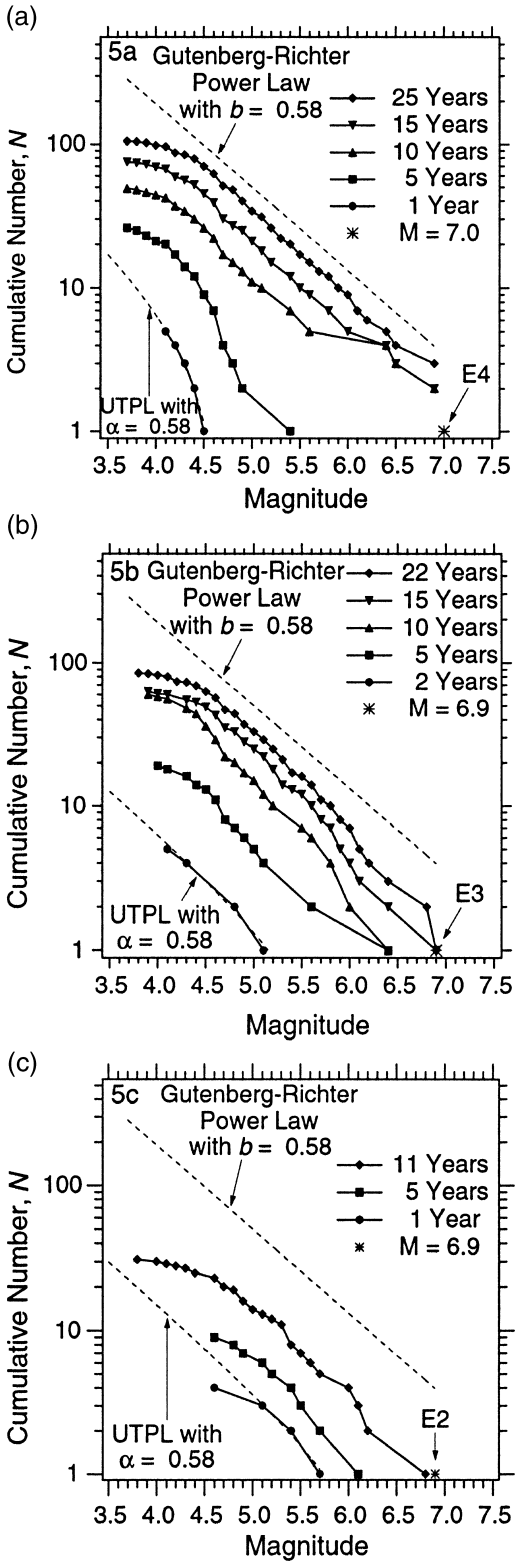

Figure 5. CFM distributions for time intervals of various lengths preceding the major earthquakes labeled in Figure 2. (a) Each curve represents the CFM distribution for all events that occurred in the indicated time interval preceding E4. The longest time interval includes all events that occurred in the 25 years preceding E4, while the shortest time interval includes only the events in the final year before E4. (b) and (c) Similar analyses for earthquakes preceding E3 and E2, respectively. These events are closer to the beginning of the data set so the time interval durations have been adjusted accordingly as indicated. The distributions for the longer time intervals have slopes consistent with a Gutenberg–Richter power law, equation (1), with a b-value of 0.58 (upper dashed line). The distributions for the shorter time intervals are consistent with an upper-truncated power law (UTPL), equation (7), with α set equal to 0.58 (lower dashed line).

creases because the occurrence of large earthquakes is less likely within a short time interval. However, short time intervals may contain large earthquakes, as seen in Figure 5. For instance, during the 10-year time interval preceding E4 (Fig. 5a), there are two earthquakes of magnitude m_b 6.9. Based on Figure 3, an earthquake of this magnitude is expected to occur once every 8.5 years. Since these two earthquakes are both sampled within the same 10-year interval, the CFM distribution does not fall off at large magnitude and fitting an upper-truncated power law would be inappropriate.

Both analysis methods show that the observed increase in slope of CFM distributions before large events is well described by an upper-truncated power law. The α-value of the upper-truncated power law determined from short time intervals is equal to the Gutenberg–Richter b-value determined from the entire record. While the b-value changes due to upper-truncation, the α-value remains constant.

Possible Causes for Temporal Variations in Maximum Magnitude

The increase in b-value observed for short time intervals before large events can be explained by temporal changes in the maximum magnitude. A fracture mechanics model for fluctuations in maximum magnitude has been proposed by Main *et al.* (1989). In their model, temporal changes in b-value can be explained by the processes of time-varying applied stress and crack growth under conditions of constant strain rate. These results were validated in the laboratory by Sammonds *et al.* (1992). Similarly, critical point systems could produce fluctuations in maximum magnitude (Main, 2000). Stress corrosion constitutive laws have also been proposed as an explanation for temporal changes in b-value and maximum magnitude (Main *et al.*, 1992). We suggest an alternate explanation for temporal changes in maximum magnitude. The long-term Gutenberg–Richter power law predicts the frequency of occurrence of earthquakes of a given magnitude. A sampling interval may or may not include the largest earthquake predicted for that interval. For example, an earthquake with a probability of occurring every 50 years may or may not be sampled in a given 50-year time interval. Various sampling intervals of the same duration will contain different maximum event sizes, thus resulting in temporal fluctuations in maximum magnitude.

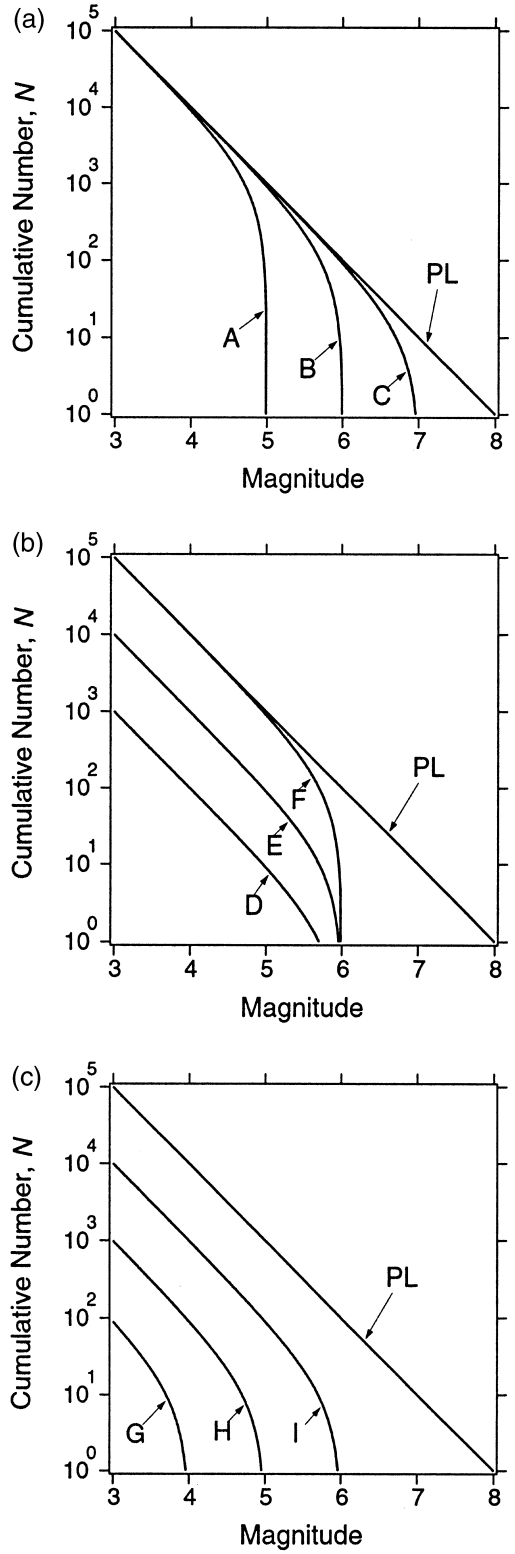

Figure 6. Upper truncation of a power law function for a cumulative distribution. The Gutenberg–Richter relation, equation (1), is shown for $a = 8$, $b = 1$ (PL). (a) The power law is upper-truncated at m_T 5, 6, and 7 (A, B, C) with $a = 8$ and $\alpha =$; 1. (b) The value of a is set equal to 6, 7, and 8 (D, E, F), while α and m_T are held constant at $\alpha = 1$ and m_T 6. (c) The value of a is set equal to 5, 6, and 7 while simultaneously setting m_T to 4, 5, and 6 (G, H, I) with $\alpha = 1$. Upper truncation of the cumulative distribution produces the observed increase in slope near the truncation magnitude. All truncated lines are plots of equation (7) with the same value of the scaling exponent, $\alpha = 1$, equal to the scaling exponent of the Gutenberg–Richter power law, $b = 1$.

Evidence from Other Regions

Tectonic Seismicity. We investigate whether or not a time-independent α-value characterizes the CFM seismicity distributions in other regions. The South American study site is the only tectonically driven seismic region that satisfies the three criteria of isolated seismicity, several large earthquakes, and a sufficient record to examine CFM distributions between the large earthquakes. Other regions of isolated seismicity are found in subduction zones, but the available record does not satisfy the second and third criteria (e.g., Indonesia and the Kuril–Kamchatka trench). For regions that satisfy the second two criteria, the seismicity is not isolated, so it is necessary to choose arbitrary geographic boundaries. Examples include regions analyzed in previous studies where temporal changes in b-value were observed (Smith, 1981, 1986; Imoto, 1991; Sahu and Saikia, 1994).

Geographic boundaries may be placed on seismic activity by the Flinn–Engdahl zoning scheme (Flinn and Engdahl, 1974; Young *et al.*, 1996). Although the criteria used to select Flinn–Engdahl (F-E) regions differ from our criteria, we can determine if a time-independent scaling parameter describes CFM distributions for F-E regions. In the USGS/NEIC PDE catalog we identify F-E regions that include a large event with a sufficient record preceding the event to examine the temporal behavior of the CFM distribution. We select four F-E regions that represent different tectonic environments: two ridge axes, the southern mid-Atlantic ridge (F-E region 410) and the Gulf of California (F-E region 49); and two subduction zones, the Kuril Islands (F-E region 221) and the New Hebrides trench southeast of the Loyalty Islands (F-E region 189).

In all four regions, we select a large event with enough earthquakes preceding the event to examine the temporal behavior of the b-value and α-value (Fig. 7, top). We apply method 2, as described above for the South American region, to examine earthquake CFM distributions in progressively shorter time intervals preceding the labeled event. We limit our analysis to earthquakes of magnitude 5 and greater because below magnitude 5 the noncumulative distributions indicate that the data set may not be complete. To determine the long-term character of the CFM distribution, we analyze the entire record for regions 410, 49, and 189 (Fig. 7a,b,d, middle). For region 221, we analyze all earthquakes preceding the event, as the number of recorded small earthquakes

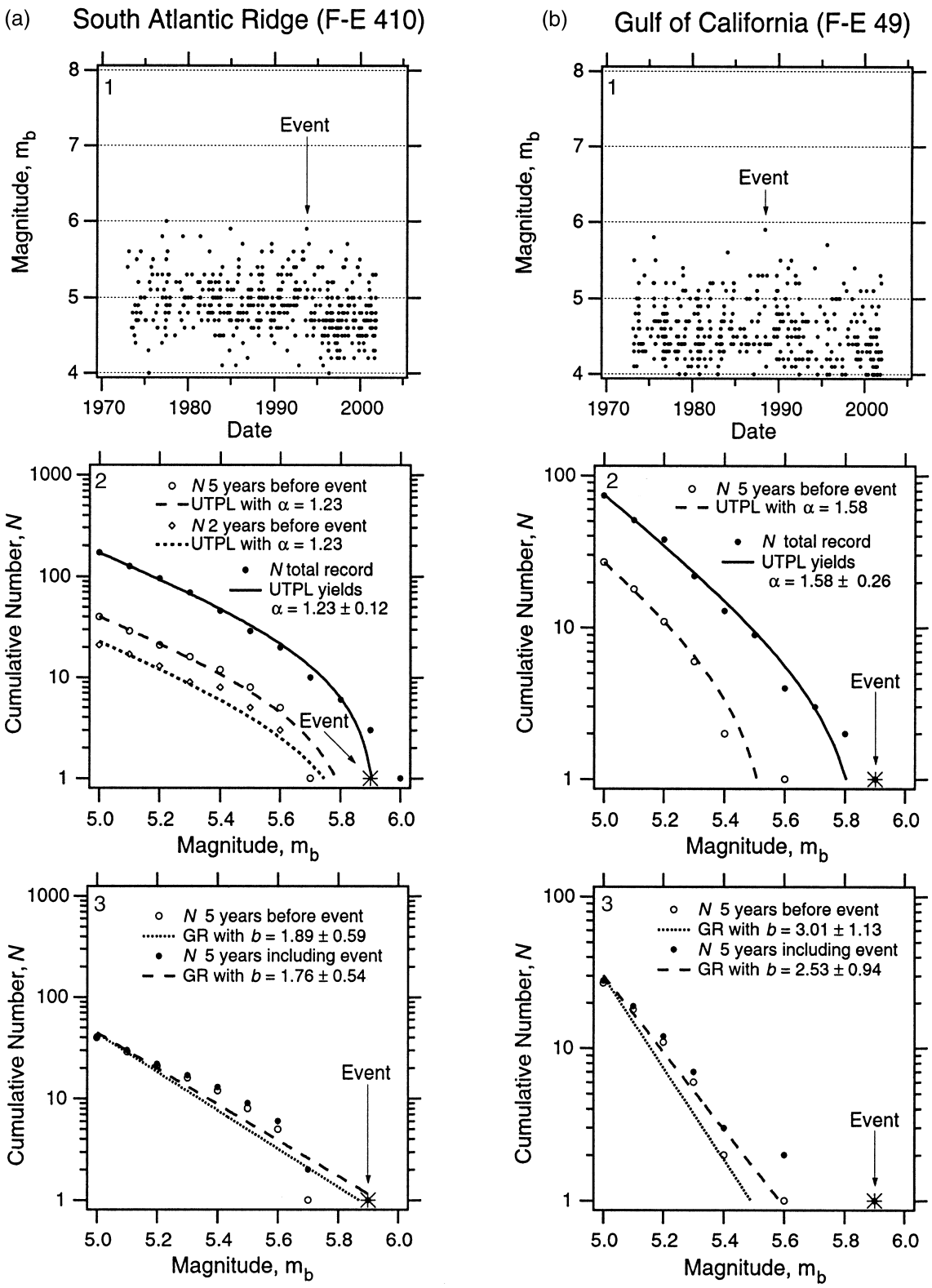

Figure 7. Analysis of regions defined by the Flinn–Engdahl (F-E) zoning scheme: (a) South-Atlantic ridge, F-E 410; (b) Gulf of California, F-E 49; (c) Kuril Islands, F-E 221; (d) New Hebrides trench, F-E 189. The top graphs, labeled 1, show earthquake magnitudes and dates. The middle graphs, labeled 2, show CFM distributions for the record shown in (1) and for various time intervals preceding the specific event. The bottom graphs, labeled 3, show CFM distributions for five years both preceding and including the event labeled in the top graphs. The *b*-values are calculated using the Aki method, equation (2). The Aki method always yields a decrease in *b*-value with the inclusion of the labeled event. All reported errors are 95% confidence limits. (*continued*)

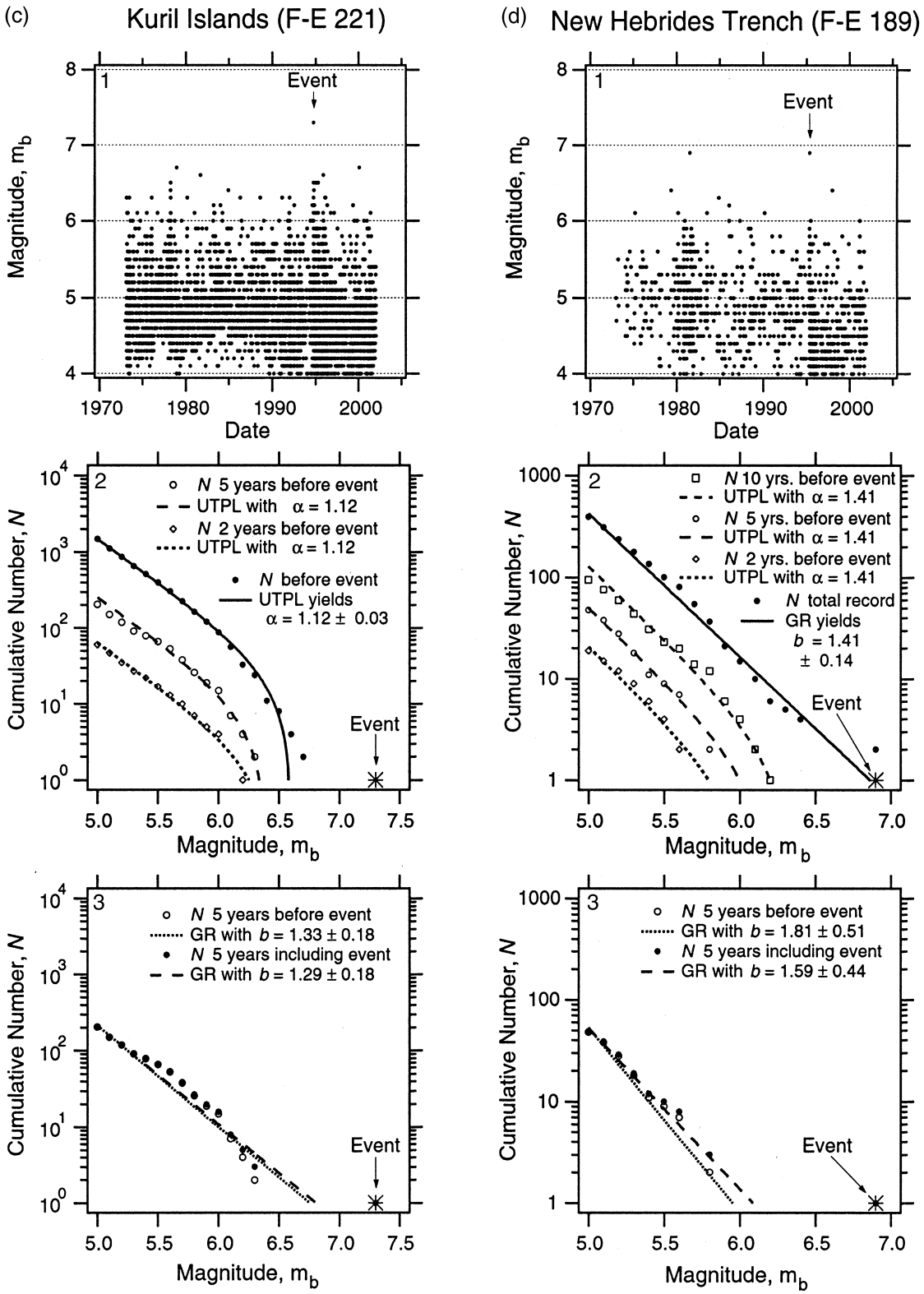

Figure 7. (*Continued*)

increases after the event (Fig. 7c, top). The long-term CFM distribution is well-described by an upper-truncated power law for regions 410, 49, and 221 (Fig. 7a–c, middle). For region 189, the long-term CFM distribution is well described by a Gutenberg–Richter power law (Fig. 7d, middle), as was seen for the Peru–Chile trench (Fig. 3). The α-values are determined by minimizing chi-square (Fig. 7a–c, middle), and the b-value is determined using the Aki method (Fig. 7d, middle). In all cases, 95% confidence levels are reported. In each region, for all time intervals analyzed, an upper-truncated power law describes the CFM distributions with the same α-value found for the long-term record (Fig. 7, middle graphs).

For the five-year time intervals, we examine the CFM distributions both preceding and including the labeled events (Fig. 7, bottom graphs). The straight lines shown in Figure 7 (bottom) are Gutenberg–Richter power laws where the Aki method is used to determine the b-values. In all four regions the occurrence of the event causes the b-value to decrease. The Aki b-value must decrease with the inclusion of any event larger than the mean magnitude (equation 2). Although the b-value varies with time, the α-value obtained from the upper-truncated power law remains constant.

Nontectonic Seismicity. Isolated seismic regions exist that are not tectonically driven. Examples include locations near volcanoes, dams, and mining operations. We illustrate how the upper-truncated power law applies to the earthquake CFM distribution from one such isolated region, Piton de la Fournaise volcano on Reunion Island in the Indian Ocean. This volcano is seismically isolated and located more than 1000 km from a plate boundary (Grasso and Bachèlery, 1995). The earthquake record consists of earthquakes recorded between 1988 and 1992 (Grasso and Sornette, 1998). Exotic events such as volcanic tremors and rock falls are not included. We find that the CFM distribution for this record is well described by an upper-truncated power law with a single scaling exponent, α, equal to 0.74 ± 0.02 (Fig. 8). Grasso and Bachèlery (1995) analyzed the CFM distribution for events that occurred between 1990 and 1992 in this region and noted that a single power law is inadequate to define the largest events. An upper-truncated power law describes the distribution with a single scaling exponent without excluding the largest events.

Upper truncation of earthquake size at the Piton de la Fournaise volcano may have several causes. Grasso and Bachèlery (1995) suggested that the fall-off at large event size is due to the limited temporal extent of the data, similar to what we observed for short time intervals of the Chile study region. Alternatively, the upper truncation may be due to physical limitations restricting the size of earthquakes in this region.

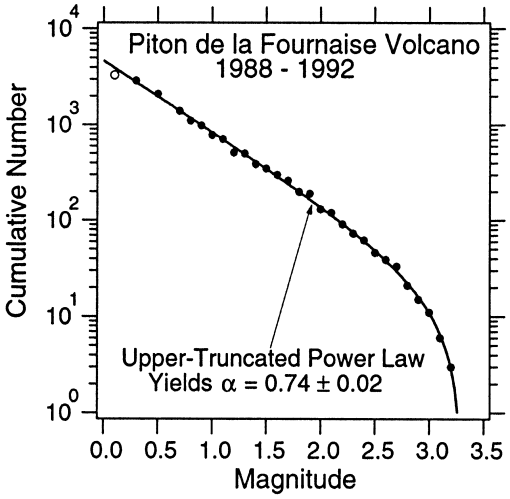

Figure 8. Cumulative frequency–magnitude distribution for earthquakes recorded between 1988 and 1992 for Piton de la Fournaise volcano (after Grasso and Sornette, 1998). Open circle is not used in analysis. An upper-truncated power law (solid line), equation (7), describes this distribution with $\alpha = 0.74 \pm 0.02$.

Summary

While it has often been observed that the b-value changes during time intervals between large earthquakes, we identify a scaling parameter that remains constant, the α-value. The b-value for short time intervals changes due to temporal changes in the maximum magnitude. An upper-truncated power law fit to an earthquake CFM distribution yields the α-value. The α-value determined for short time intervals is equal to the Gutenberg–Richter b-value determined from longer records. While the b-value changes due to upper-truncation, the α-value remains constant and may be used for long-term probabilistic forecasting.

Acknowledgments

We thank C. Barton and D. Naar for critical reviews of an early version of this manuscript. We thank editor A. Michael, reviewer I. Main, and one anonymous reviewer for constructive criticism that improved this manuscript. The earthquake data were obtained from the USGS NEIC/PDE website (http://wwwneic.cr.usgs.gov/neis/epic/epic_global.html).

References

Aki, K. (1965). Maximum likelihood estimate of b in the formula $\log N = a - bM$ and its confidence limits, *Bull. Earthquake Res. Inst. Univ. Tokyo* **43,** 237–239.

Bender, B. (1983). Maximum likelihood estimation of b values for magnitude grouped data, *Bull. Seism. Soc. Am.* **73,** 831–851.

Burroughs, S. M., and S. F. Tebbens (2001a). Upper-truncated power law distributions, *Fractals* **9,** 209–222.

Burroughs, S. M., and S. F. Tebbens (2001b). Upper-truncated power laws in natural systems, *Pure Appl. Geophys.* **158,** 741–757.

Cosentino, B., V. Ficarra, and D. Luzio (1977). Truncated exponential frequency-magnitude relationship in earthquake statistics, *Bull. Seism. Soc. Am.* **67,** 1615–1623.

Fiedler, B. G. (1974). Local b-values related to seismicity, *Tectonophysics* **23,** 277–282.

Field, E. H., D. D. Jackson, and J. F. Dolan (1999). A mutually consistent seismic-hazard source model for southern California, *Bull. Seism. Soc. Am.* **89,** 559–578.

Flinn, E. A., and E. R. Engdahl (1974). Seismic and geographical regionalization, *Bull. Seism. Soc. Am.* **64,** 771–993.

Grasso, J.-R., and P. Bachèlery (1995). Hierarchical organization as a diagnostic approach to volcano mechanics: Validation on Piton de la Fournaise, *Geophys. Res. Lett.* **22,** 2897–2900.

Grasso, J.-R., and D. Sornette (1998). Testing self-organized criticality by induced seismicity, *J. Geophys. Res.* **103,** 29965–29987.

Guha, S. K. (1979). Premonitory crustal deformations, strains and seismotectonic features (*b*-values) preceding Koyna earthquakes, *Tectonophysics* **52,** 549–559.

Gutenberg, B., and C. F. Richter (1949). *Seismicity of the Earth and Associated Phenomena*, Princeton University Press, Princeton, New Jersey.

Imoto, M. (1991). Changes in the magnitude-frequency *b*-value prior to large ($M \geq 6.0$) earthquakes in Japan, *Tectonophysics* **193,** 311–325.

Kagan, Y. Y. (1991). Seismic moment distributions, *Geophys. J. Int.* **106,** 123–134.

Kagan, Y. Y. (1993). Statistics of characteristic earthquakes, *Bull. Seism. Soc. Am.* **83,** 7–24.

Main, I. (2000). Apparent breaks in scaling in the earthquake cumulative frequency-magnitude distribution: fact or artifact? *Bull. Seism. Soc. Am.* **90,** 86–97.

Main, I., J. R. Henderson, P. G. Meredith, and P. R. Sammonds (1994). Self-organised criticality and fluid-rock interactions in the brittle field, *Pure Appl. Geophys.* **142,** 529–543.

Main, I. G., P. G. Meredith, and C. Jones (1989). A reinterpretation of the precursory seismic *b*-value anomaly from fracture mechanics, *Geophys. J.* **96,** 131–138.

Main, I. G., P. G. Meredith, and P. R. Sammonds (1992). Temporal variations in seismic event rate and *b*-values from stress corrosion constitutive laws, *Tectonophysics* **211,** 233–246.

Molchan, G. M., and O. Dmitrieva (1990). Dynamics of the magnitude-frequency relation for foreshocks, *Phys. Earth Planet. Inter.* **61,** 99–112.

Molchan, G. M., T. L. Kronrod, and A. K. Nekrasova (1999). Immediate foreshocks: time variation of the *b*-value, *Phys. Earth Planet. Inter.* **111,** 229–240.

Olami, Z., H. J. S. Feder, and K. Christensen (1992). Self-organized criticality in a continuous, non-conservative cellular automaton modeling earthquakes, *Phys. Rev. Lett.* **68,** 1244–1247.

Oncel, A. O., T. H. Wilson, and O. Nishizawa (2001). Size scaling relationships in the active fault networks of Japan and their correlation with Gutenberg–Richter *b* values, *J. Geophys. Res.* **106,** 21,827–21,841.

Page, R. (1968). Aftershocks and microaftershocks of the great Alaska earthquake of 1964, *Bull. Seism. Soc. Am.* **58,** 1131–1168.

Sahu, O. P., and M. M. Saikia (1994). The *b* value before the 6th August, 1988 India-Myanmar border region earthquake—a case study, *Tectonophysics* **234,** 349–354.

Sammonds, P. R., P. G. Meredith, and I. G. Main (1992). Role of pore fluids in the generation of seismic precursors to shear fracture, *Nature* **359,** 228–230.

Smith, W. D. (1981). The *b*-value as an earthquake precursor, *Nature* **289,** 136–139.

Smith, W. D. (1986). Evidence for precursory changes in the frequency-magnitude *b*-value, *Geophys. J. R. Astr. Soc.* **86,** 815–838.

Utsu, T. (1965). A method for determining the value of b in a formula log $n = a - bM$ showing the magnitude-frequency relation for earthquakes (with English summary), *Geophys. Bull. Hokkaido Univ.* **13,** 99–103.

Working Group on California Earthquake Probabilities (1995). Seismic hazards in southern California: probable earthquakes, 1994 to 2024, *Bull. Seism. Soc. Am.* **85,** 379–439.

Young, J. B., B. W. Presgrave, H. Aichele, D. A. Wiens, and E. A. Flinn (1996). The Flinn-Engdahl regionalisation scheme: the 1995 revision, *Phys. Earth Planet. Inter.* **96,** 223–297.

University of South Florida
College of Marine Science
St. Petersburg, Florida 33701
sburroughs@ut.edu
tebbens@marine.usf.edu
(S.M.B., S.F.T.)

University of Tampa
Department of Chemistry and Physics
Tampa, Florida 33606
(S.M.B.)

Manuscript received 2 July 2001.